Springer

KSME

Journal of Mechanical Science and Technology 24 (9) (2010) 1799~1807
www.springerlink.com/content/1738-494x
DOI 10.1007/s12206-010-0630-y

One-pitch passage designed inversely with a single blade for cascade experiments †

Chong-Hyun Cho[1], Kook-Young Ahn[2], Young-Cheol Kim[2] and Soo-Yong Cho[1,*]

[1]*Department of Mechanical and Aerospace Engineering(RECAPT), Gyeongsang National University, Jinju, 660-701, Korea*
[2]*Department of Eco-Machinery Korea Institute of Machinery and Materials, Daejeon, 305-343, Korea*

(Manuscript Received February 23, 2009; Revised April 26, 2010; Accepted May 18, 2010)

Abstract

A linear cascade experimental apparatus often consists of only a few cascade blades. Advantages to this experimental arrangement are increased by the use of larger cascade blades, a lower mass flow rate, a corresponding decrease in required power, and easier optical access within the cascade passage. However, fewer cascade blades in the cascade row make it difficult to establish periodic flow conditions between blades compared to infinite cascade model experiments. Generally, removing fluid from the cascade walls or adjusting tailboards located downstream of the cascade are common methods to establish periodic flow conditions through the cascade blades. In this study, a passage for cascade experiments is designed to satisfy infinite cascade flow conditions without any flow control or tailboards. A one-pitch at cascade row is adopted as its width and only a single cascade blade is installed within the passage. The surface isentropic Mach number distribution on the blade is chosen for the existence of infinite cascade flow conditions, and 14 geometric design variables related to the passage shape are applied to the design of a one-pitch passage by using a genetic algorithm. Flow structures within a passage designed using a genetic algorithm match with those obtained with the infinite cascade flow condition. Computed results obtained with a single cascade blade show that infinite cascade flow conditions can be obtained by modifying only the passage walls of the cascade experimental apparatus.

Keywords: Cascade; Turbomachinery; Inverse design; Optimization; Compressible flow

1. Introduction

Experiments on turbine cascades have produced many important findings [1-3] on such things as separation mechanisms on blade surfaces, flow structures within a passage, and unsteady effects of wakes, etc. Today, computational fluid dynamics (CFD) techniques are widely used to capture more detailed flow physics and design more efficient gas turbine engine components [4-7]. However, in flow fields sensitive to turbulence properties such as film cooling or heat transfer rates [8], CFD provides diverse results depending on the turbulence model used. For these cases, cascade experiments would be more reliable; they also provide a better flow field for understanding turbulence properties, the effect of convex and concave curvature of blades, and stagnant point anomaly, and so on.

Full rotating rigs have been used to acquire unsteady flow fields on a rotating turbine. Giess and Kost [9] measured flow fields in a rotating annular turbine cascade using pneumatic probes and pressure taps. Recently, PIV has been widely used to measure unsteady three-dimensional velocity fields in rotating rigs to investigate such phenomena as blade row interaction between a turbine stator and rotor, flows in shrouded cavities affected by axial turbine, and unsteady flows within a compressor passage [10-12]. Such tests are more costly and require more complicated measuring devices. One particular challenge is the transmission of sheet forming optics to capture the desired flow fields within a blade passage. This problem can be avoided if cylindrical bars traversing across the inlet flow are applied to linear cascades to simulate the wakes of an actual blade row. With wake simulators, unsteady flow phenomena, such as the convection of a turbulent wake through a low pressure turbine cascade and interaction between the wake and a separation bubble etc., were measured [13-15].

Linear and annular cascades have been used as an alternative to rotating rigs. Linear cascades provide better spatial resolution than full annulus cascades for the same flow rate, and also provide good mid-span data. However, linear cascade experiments should ensure periodic flow conditions between cascade blades ideally as infinite cascade flow conditions. To obtain periodic flow conditions, the operating gas may be

† This paper was recommended for publication in revised form by Associate Editor Won-Gu Joo

* Corresponding author. Tel.: +82 55 751 6106, Fax: +82 55 757 5622
E-mail address: sycho@gnu.ac.kr

removed from the cascade walls and tailboards located downstream of the cascade could be adjusted. These options require many intricate works in side-zones of the cascade row. Additionally, the effect of upstream boundary layers should be removed so that infinite cascade flow conditions can exist at the tested cascade blades. Conducting cascade experiments with only a single cascade blade not only improves optical access but also reduces the required flowrate for blade of the same size. However, with regard to establishing infinite cascade flow conditions, the use of a single blade causes more difficulties than cascades with multiple blades. Flow conditions within a passage where a single cascade blade is installed could be very sensitive to the bleeding rate of suction air and the suction device could interfere with optical access.

Building a linear cascade experimental apparatus that does not require suction bleeds or adjustable tailboards to create infinite cascade flow conditions would be very beneficial. Laskowski et al. [16] designed a passage for a linear cascade experiment: they used a gradient-based optimization method to obtain an infinite cascade flow condition without the use of suction bleeds. The width of the passage was double-pitch and only a single-cascade blade was installed within the passage. However, Mach number contours within the passage showed some discrepancy between the computed results obtained with an infinite cascade flow condition and the results obtained with the designed double-pitch passage because the flow within the passage was sensitive to the passage wall shape.

When flow structures around a single blade are matched well with the flow structures obtained with an infinite cascade flow condition, they not only improve the accuracy of experiment but also provide correct physical phenomena. In this study, a one-pitch passage is designed with a single-cascade blade. For the design, a genetic algorithm is used to ensure the same flow structures exist around the blade as infinite cascade. Fourteen design variables related to the passage are used to adjust the wall shape. The flow structures within the passage designed with the genetic algorithm is compared to those obtained by infinite cascade flow conditions. The surface Mach number distribution on the cascade blade is also compared to the experimental results [17].

2. Design variables

2.1 Initial wall shape

The experiment conducted by Kiock et al. [17] was adopted for the desired basic flow structure on a linear turbine cascade operating under an infinite cascade flow condition. Their experiment used typical cooled gas turbine rotors to investigate the effect of wind tunnel environment on the test results of four European wind tunnels using different test sections. The experimental conditions which varied slightly for each experiment are shown in Table 1. The experimental results are shown in section 4 together with the computed result of this study.

For the cascade shown in Fig. 1, the computational domain

Table 1. Experimental conditions on the four different wind tunnel facilities [17].

Parameters	RG	GO	BS	OX
Chord (mm)	32.6	60	100	100
Aspect ratio	1.534	2.083	3.000	3.000
Pitch (mm)	25.13	42.58	70.88	70.88
Stagger angle	33.14°	33.56°	33.29°	33.29°
Inlet flow angle	28.95°	29.92°	29.92°	30.04°
Exit flow angle	67.03°	67.02°	67.33°	67.76°
Turbulence intensity	1%	1%	0.3-0.6%	<1%

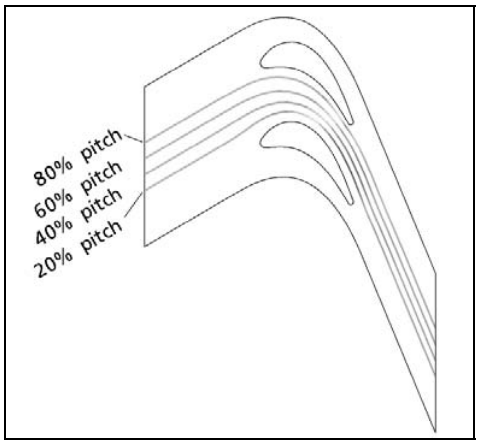

Fig. 1. Streamlines at different locations within a cascade passage.

along the blade pitch was created so that the upper boundary (near the suction surface of the upper blade) was selected on the basis of the double-pitch from the lower boundary (near the pressure surface of the lower blade). This domain was easily calculated because periodic boundary conditions could be applied to both boundaries. In the computation of a double-pitch cascade with an infinite periodic cascade flow condition, the lower boundary could be selected arbitrarily and the upper boundary was defined as two blade pitches away from the lower boundary. Fig. 1 shows a computational domain which is formed by this method.

A one-pitch passage for cascade experiments consists of sidewalls (an upper wall and a lower wall). If initial sidewalls are simply designed without any consideration of the flow through blade passages, more computation time is needed to reach the same flow structure so that obtained using the infinite cascade flow condition. Additionally, the final flow structure obtained with an optimization method could tend to produce a locally optimized result which depends on the initial wall shape. For a more reasonable initial sidewall shape, the wall shape may be designed by using a streamline along the wall surface. Thus, any abrupt changes to the flow within the passage are eliminated and the computed flows obtained through the optimization method can match the desired flow structure at a faster rate.

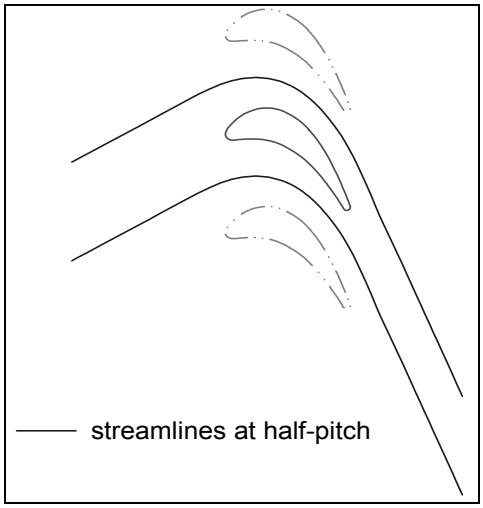

Fig. 2. Initial wall profiles obtained from streamlines at a 50% pitch.

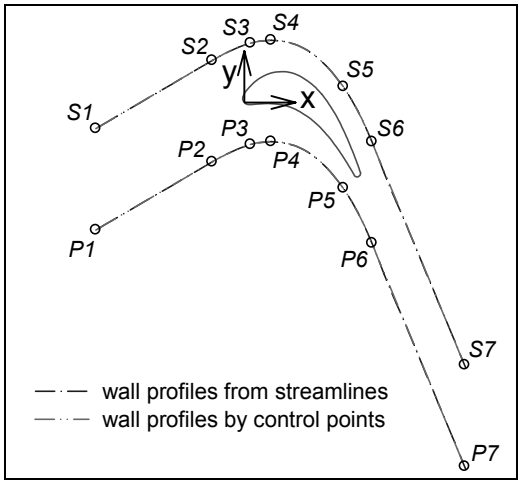

Fig. 3. Control points on the upper and lower walls to modify wall shapes.

Fig. 1 shows four different streamlines located within the cascade passage. They were located at a pitch of 20%, 40% 60% and 80% from the lower blade. The streamline at a 50% pitch was applied to the initial shape of the lower wall and the upper wall for a one-pitch cascade model. Fig. 2 shows the computational domain of the one-pitch passage installing a single cascade blade.

2.2 Selection of design variables

Even though the sidewalls are designed on the basis of the streamlines, flow structures within the passage may differ from the flow structures obtained with a periodic flow condition (or an infinite cascade flow condition) because boundary layers along the sidewalls influence the flow in the one-pitch passage. These sidewalls should therefore be adjusted to obtain the same flow structure on a cascade blade as that which would be obtained with a periodic flow condition. Control points are used to change the sidewall shape. Seven control points are applied on both the upper and lower walls. A third-order polynomial or linear curve fit is then used to define the surface between the control points. A few control points can be chosen as design variables and used to adjust the wall shape.

The control points on the sidewall are shown in Fig. 3. Values of the y-location of the control points are defined by the streamline. The x-location of point 1 ($S1_X$, $P1_X$) was selected as 120% of the blade chord upstream from the leading edge, and point 2 ($S2_X$, $P2_X$) was 25% of the blade chord upstream of the leading edge. Point $S3_X$ was downstream from the leading edge by 20% of the chord that is created between the leading edge and a peak point on the upper wall. As with $S3_X$ point $P3_X$ was selected, but a peak point was selected on the lower wall. The reason for this selection was because the flow direction was changed after it passed the leading edge due to the blade thickness, and these points (*S3*, *P3*) were used to capture this phenomenon.

Point 4 (*S4*, *P4*) was selected at a peak location on the streamline. Point 5 (*S5*, *P5*) was defined similar to point 3 to catch the flow change at the aft blade section. Point $S5_X$ was selected upstream from the trailing edge by 20% of the chord that is created a line between the trailing edge and the peak point on the upper wall, and the point of $P5_X$ was selected by the same method as the point of $S5_X$ except for the peak point on the lower wall. Point 6 (*S6*, *P6*) was chosen as 25% of the blade chord downstream from the trailing edge along the exit flow direction, and point 7 (*S7*, *P7*) was located at 200% of the blade chord downstream from the trailing edge.

The shape between control point 6 and control point 7 was formed by using a straight line because they are located in the outlet region. Other control points were connected by using the third-order polynomial curve. For the formation of a smooth shape between control points, the gradients at the control points should be set to the same when two segments are connected at a common point. Point 1 (*S1*, *P1*) and point 2 (*S2*, *P2*) were fixed because they were defined on the basis of the one-pitch and were located at the inlet region. The y-locations for point 3, point 5 and point 6 could be changed to control the wall shape, but the x-locations for the same points remained fixed as initially determined. The gradients on point 3 and point 5 could be changed to control the wall shape between point 2 and point 4 and the wall shape between point 4 and point 6, respectively. Point 4 was selected to control the peak locations on the sidewalls. Therefore, even though the x-location and y-location of point 4 could be changed, its gradient was fixed to zero. The y-location for point 7 ($S7_Y$, $P7_Y$) could be changed, but they were not control points because they depended on the point 6 and the exit flow angle. From these adjustable variables for the sidewall shape, seven control points are chosen for defining the upper and lower walls. Table 2 shows these 14 control points which are used to adjust the wall shape in the passage design process.

Using this method, values for the control points can be obtained from the wall shape that is formed by the streamlines.

Table 2. 14 design variables to modify the upper and lower wall.

	Design variables
upper wall	y at control point S3 ($S3_Y$) angle at control point S3 ($S3_\theta$) x at control point S4 ($S4_X$) y at control point S4 ($S4_Y$) y at control point S5 ($S5_Y$) angle at control point S5 ($S5_\theta$) y at control point S6 ($S6_Y$)
lower wall	y at control point P3 ($P3_Y$) angle at control point P3 ($P3_\theta$) x at control point P4 ($P4_X$) y at control point P4 ($P4_Y$) y at control point P5 ($P5_Y$) angle at control point P5 ($P5_\theta$) y at control point P6 ($P6_Y$)

Table 3. Values of control points obtained from the streamline on the upper and lower wall.

Control points	x location (x/c)	y location (y/c)	angle
S1	(-1.039)	(-0.201)	(30.0)
S2	(-0.216)	(0.276)	(30.0)
S3	(0.055)	0.398	14.97
S4	0.202	0.418	(0.0)
S5	(0.712)	0.092	-54.99
S6	(0.915)	-0.293	(-67.18)
S7	(1.571)	(-1.856)	(-67.18)
P1	(-1.039)	(-0.911)	(30.0)
P2	(-0.216)	(-0.434)	(30.0)
P3	(0.055)	-0.312	14.97
P4	0.202	-0.292	(0.0)
P5	(0.712)	-0.618	-54.99
P6	(0.915)	-1.003	(-67.18)
P7	(1.571)	(-2.566)	(-67.18)

( ): remains fixed during inverse design

These values are shown in Table 3. The values in brackets are obtained as control points, but they do not change during the sidewall design. Fig. 3 shows a comparison between the streamlines and the wall shapes designed with the control points shown in Table 3. The wall shapes are well matched to the streamlines. Since the wall shapes obtained using control points match well with any streamlines located within the cascade passage, the control points selected by this method have high flexibility on the sidewall design and they can be applied as design variables to control the wall shape in the inverse design process.

3. Optimization and flow analysis algorithm

3.1 Objective function and constraints

The goal of this study was to obtain an infinite cascade flow condition in a single cascade model even though boundary condition is defined by the wall and not periodic. The surface isentropic Mach number distribution (SIMN; τ) obtained with the periodic flow condition is chosen as a target, and the difference between the SIMN obtained using the periodic flow condition and the SIMN obtained using a wall boundary condition was minimized. Thus, the difference between the two SIMNs becomes an objective function as follows:

$$Minimize: obj = H^*(\vec{X}) \quad \text{at} \quad \Gamma_{suc} \quad \text{and} \quad \Gamma_{pre} \tag{1}$$

where H^* and $\vec{X}$ are the objective function and design variables, respectively. Γ_{suc} refers to the suction surface of the blade and Γ_{pre} refers to the pressure surface.

As a constraint on the design variables, point 3 should be located between point 2 and point 4 because point 4 is the peak location on the wall geometry. Point 5 should also be located between point 4 and point 6 in a similar fashion as point 3. The upper wall shape was restricted so that it did not make contact with the suction surface of the blade. Furthermore, the pressure surface of the blade should be located above the lower wall geometric definition. These requirements can be achieved by restricting $S3_Y$, $S4_Y$ and $S5_Y$ to be located above the suction surface of the blade, and also by restricting $P3_Y$, $P4_Y$ and $P5_Y$ to be located below the pressure surface of the blade. Point 4 was located between point 3 and point 5 in the x-direction. However, these constraints were more limited when the objective function was seriously deteriorated over the bounds as shown in Table 4. The gradient of point 3 and point 5 were adjustable, but the lower and upper bound were limited so that the wall shape was not twisted.

Table 4. Constraints of design variables.

Design variables	Lower bounds (Γ)	Upper bounds (Γ)
$S3_Y$	Max($S2_Y$, 0.362)	Max($S4_Y$, 0.404)
$S3_\theta$	13.3	16.3
$S4_X$	Max($S3_X$, 0.172)	Max($S5_X$, 0.231)
$S4_Y$	Max(max($S3_Y$, $S5_Y$) , 0.405)	0.450
$S5_Y$	Max($S6_Y$, 0.065)	Max($S4_Y$, 0.125)
$S5_\theta$	-55.5	48.0
$S6_Y$	Max($S7_Y$, -0.318)	Max($S5_Y$, -0.268)
$P3_Y$	Max($P2_Y$, -0.332)	Max($P4_Y$, -0.306)
$P3_\theta$	18.2	22.4
$P4_X$	Max($P3_X$, 0.181)	Max($P5_X$, 0.229)
$P4_Y$	Max(max($P3_Y$, $P5_Y$) , -0.305)	-0.279
$P5_Y$	Max($P6_Y$, -0.616)	Max($P4_Y$, -0.550)
$P5_\theta$	-55.2	50.0
$P6_Y$	Max($P7_Y$, -0.102)	Max($P5_Y$, -0.980)

3.2 Optimization algorithm

Optimization is a procedure that seeks optimal values for

design variables; those values should lead to the best objective function (such as minimization, maximization, or targeting) without violating constraints. A gradient-based method is generally the most appropriate if there are more than 10 design variables. This method usually does not require many calculations to reach a target compared to the response surface method or the genetic algorithm. However, gradient-based methods cannot guarantee the optimum values of the objective function throughout the entire design region. Cho et al. [18] showed a gradient-based method could not obtain the best optimum value for the objective function throughout the entire design region on the inverse design for a 160% pitch passage with a single blade although the initial wall shapes were designed carefully with streamlines. Since the flow structures on the suction of the blade were sensitive in the experiment [17], and the gradient-based method could not guarantee the optimum of the objective function, a genetic algorithm in the VisualDOC [19] was adopted for the inverse design. The population was selected as 100 for a generation. The cross-over probability and mutation were chosen as 95% and 10%, respectively.

3.3 Computational method

For calculating the two-dimensional compressible turbulent flow field within the one-pitch passage, CFX-11 [20] was used. A high resolution, which is more accurate than a second order, was applied for the discretization, and Menter's two-equation turbulence model (SST) was used for turbulence calculation. An unstructured grid was used, and the computed results were the same when more than 120,000 elements were applied in the computational domain. For this computation, more than 150,000 elements were used in the computational domain, and the first grid away from the wall had a y+ near 1. The computational domain extended the 120% blade chord upstream and downstream by 200% of the blade chord. Convergence was achieved when all residuals dropped at least 10 to the seventh orders in magnitude.

Fig. 4 shows the inverse design process. The sidewalls are modified during the optimization with new design variables, and the objective function of the isentropic surface Mach number is obtained in the post-process after the computation completed. This process is iterated until the objective function is minimized. Boundary conditions are given in the pre-process. In this study, the width of the passage was fixed to the one-pitch at inlet. Therefore, two different boundary conditions can be applied to this problem. In the first condition, the same mass flowrate used in the infinite cascade model is applied to the inlet flow condition with the static pressure condition at exit; in the second condition, the total pressure and static pressure obtained in the infinite cascade model can be applied to the inlet and exit flow condition, respectively. In the test of two different boundary conditions with the genetic algorithm, the SIMN on the blade was identical and the inverse designed sidewalls were expanded compared to the initial wall shape. The mass flowrate was reduced by only 0.08% when the total pressure was applied to the inlet flow condition.

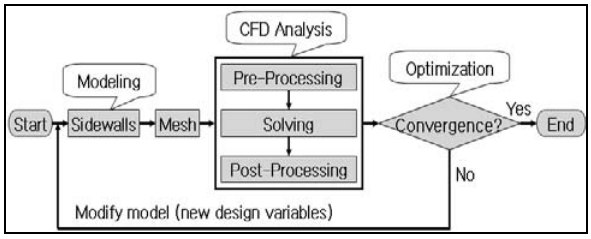

Fig. 4. Flowchart for the inverse design process connected with the CFD.

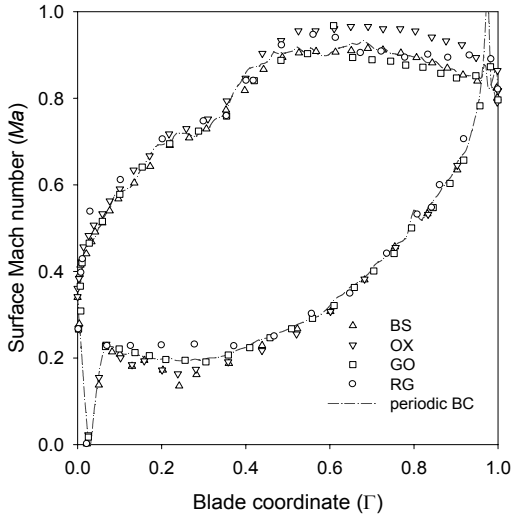

Fig. 5. Comparison of the SIMN obtained with the periodic flow condition and the experimental data.

4. Results and discussion

4.1 Comparison with experimental data

Following a review of the four different experimental conditions shown in Table 1, the inlet flow angle and exit flow angle were selected to be 30° and 68°, respectively. The pitch-to-chord ratio was chosen as 0.71 and the turbulence intensity at inlet was set to 0.5% in the model. Fig. 5 shows a computed result compared with the experimental data. This computed result was obtained with a periodic flow condition and the SIMN was computed by using the total pressure at inlet and the static pressure on the blade surface. The experimental data are indicated by marks which show four different results and the computed result is expressed with lines. The experi- mental results show that the flow structures on the suction surface of the cascade blade were sensitive; furthermore, some experimental uncertainty was generated by the different experimental environment.

4.2 Inverse design

The computed result in the one-pitch passage which is

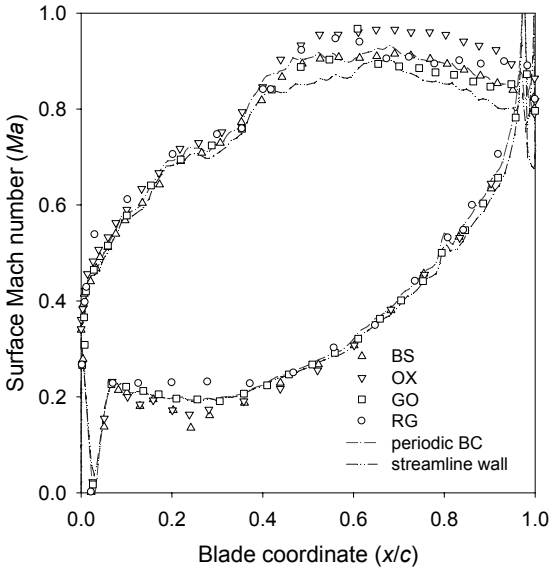

Fig. 6. Comparison of the SIMN when streamlines are used as the sidewalls of the passage.

changed to a wall from the streamlines is shown in Fig. 6. Although the sidewalls were developed from the streamlines, the flow was changed because of the growth of the boundary layer along the sidewalls. Note In particular that in contrast with the SIMN obtained with the periodic flow condition, the discrepancy on the suction surface increased. The sidewalls should therefore be changed by using the design variables in order to obtain the same flow structure that is computed with the periodic flow condition through the inverse design procedure. In this case, the SIMN of the experimental data can be applied to an objective function instead of the simulated SIMN computed with a periodic flow condition. However, in practice sidewalls are generally designed before the experimental result are known. The computed SIMN ($\tau_{\inf}$) obtained with the periodic flow condition is therefore chosen for a target flow structure in this inverse design.

In the evaluation of the objective function during the optimization process, unrealistic results were generated near the leading edge of the pressure surface as well as near the trailing edge due to grids or stagnation point. The evaluation range for the objective function was limited to 0.01-0.95 on the suction surface and 0.08-0.95 on the pressure surface so that ranges could be avoided where the SIMN was exaggerated in the evaluation of the objective function. A weighting function was applied to the objective function on the suction surface as follow:

$$H^* = \omega_1 \left| \int_{0.01}^{0.95} \tau_{suc} d\Gamma_{suc} - \int_{0.01}^{0.95} \tau_{\inf} d\Gamma_{suc} \right| + \omega_2 \left| \int_{0.08}^{0.95} \tau_{pre} d\Gamma_{pre} - \int_{0.08}^{0.95} \tau_{\inf} d\Gamma_{pre} \right| \quad (2)$$

where τ_{suc} and τ_{pre} are the SIMN along the suction surface and the pressure surface of the blade, and ω_1 and ω_2 are

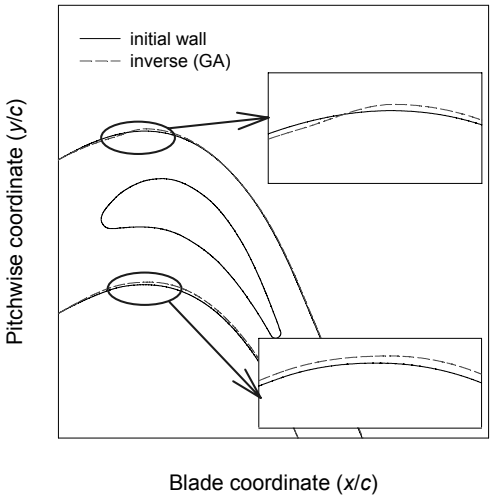

Fig. 7. Comparison of sidewall profiles obtained with the genetic algorithm.

weighting functions set to 1.5 and 1.0, respectively. The value of ω_1 is larger so that accurate results can be obtained on the suction surface.

A genetic algorithm was applied to the inverse design process to reach an optimum objective function throughout the entire design region. Fig. 7 shows the sidewalls designed with the genetic algorithm from the initial walls designed using the streamlines. Since the passage of the initial walls showed the lower SIMN on the suction surface of the blade than the SIMN obtained under the periodic flow condition, the walls would be designed to increase this low SIMN on the suction surface at the aft blade section through the optimization process. Therefore, the inverse designed lower wall moves up at the blade section to shrink the passage. At the upper wall, it moves down at the fore blade section and slightly moves up at the aft blade section. However, the width of the passage is expanded and the SIMN on the suction surface is correspondingly increased at the aft blade section. In particular, the movement of the peak y-location of the upper wall soothes the effect of boundary layer growth on the sidewall due to the expansion of the passage.

Table 5 shows the values of the design variables on the inversed designed sidewalls. Since the flow structure on the suction surface was sensitive to the variation of the sidewalls, the x-location and y-location of the design variables which ware non-dimensionalized by the blade chord were subdivided into $O(10^{-4})$ and the angles into $O(10^{-2})$. Fig. 8 shows a comparison of the SIMN obtained in the passage designed using the genetic algorithm with the target SIMN. The SIMN on the pressure surface agrees well with the target SIMN obtained with the periodic flow condition but The SIMN on the pressure surface on the suction surface shows some discrepancy for the target SIMN.

In the inverse design of the sidewalls on a double-pitch passage where double cascade blades were installed, Cho et al. [21] showed that the SIMN on the blade surface matched well

Table 5. Value of design variables when the sidewalls are optimized using the genetic algorithm.

Variables	x location (x/c)	y location (y/c)	angle
S3	-	0.3890	16.13
S4	0.2042	0.4285	-
S5	-	0.0951	-53.96
S6		-0.2850	-
P3	-	-0.3077	19.67
P4	0.2242	-0.2798	-
P5	-	-0.5792	-53.30
P6	-	-1.0002	-

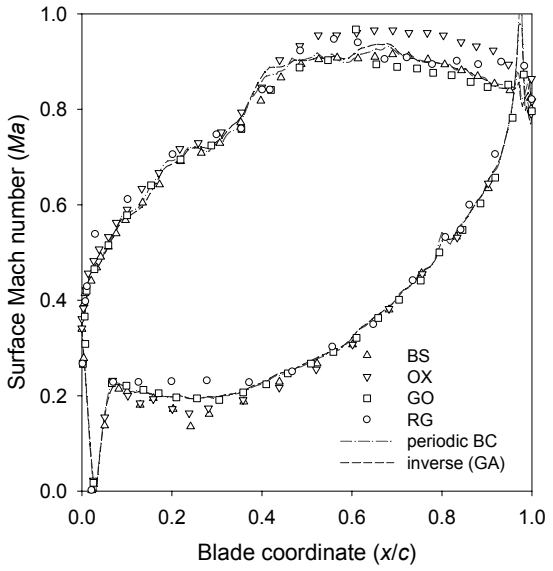

Fig. 8. Comparison of the SIMN obtained in the passage designed by the genetic algorithm and the target SIMN.

with the target SIMN even though a gradient-based method was applied in the optimization process. This optimum objective function throughout the entire design region was obtained since the passage between two blades was protected against the boundary layer growth on the sidewalls by each blade. However, the flow structures in a passage installed a single blade are directly affected by the sidewalls of the passage. This means that the genetic algorithm is more appropriate for the inverse design of the passage installing a single blade than the gradient based method, and a better matched SIMN on the suction surface could be obtained by applying more design variables.

Fig. 9(a) shows how the objective functions changed at each generation, which required 45 generations to reach a convergence. Fig. 9(b) shows the variation of all objective functions during the inverse design procedures which were iterated 4500 times. In the optimization process, the objective function on the suction surface was bigger than that on the pressure surface. This resulted from the sensitivity of the flow

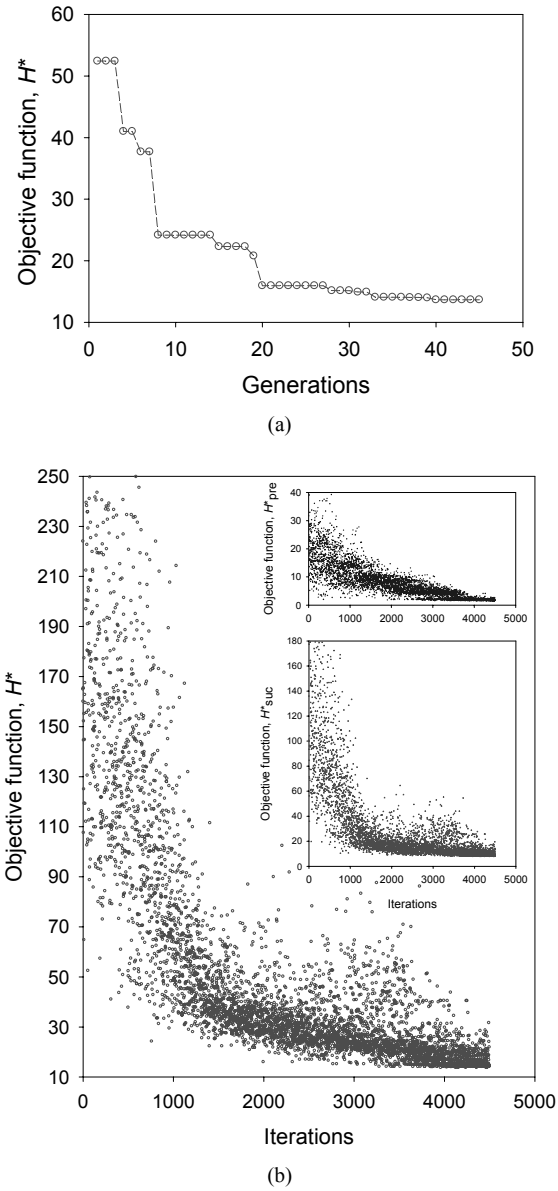

Fig. 9. Convergence history of the objective functions in the optimization process with the genetic algorithm (a) at each generation (b) overall iterations.

structure on the suction surface according to the variation of the sidewalls. Therefore, the objective function on the suction surface was weighted by 1.5 times than that on the pressure surface. The objective function that was converged by means of the genetic algorithm showed 84% greater improvement than the objective function obtained from the initial wall.

A comparison of Mach number contours in the cascade passage is shown in Fig. 10. The Mach number contours in the passage obtained with the genetic algorithm agree well with those of the computed result obtained with the periodic flow boundary condition. In particular, the Mach number contours at the aft of the blade near the suction surface in the inverse designed passage are greatly improved compared with those within the passage of the initially designed wall.

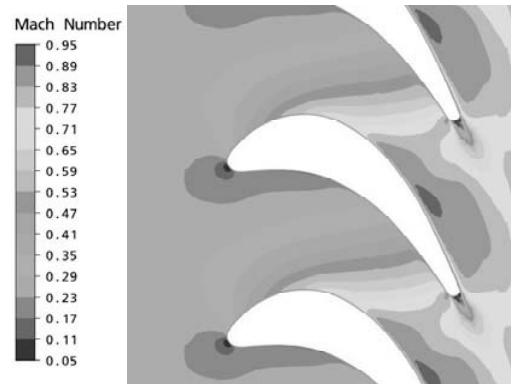

(a)

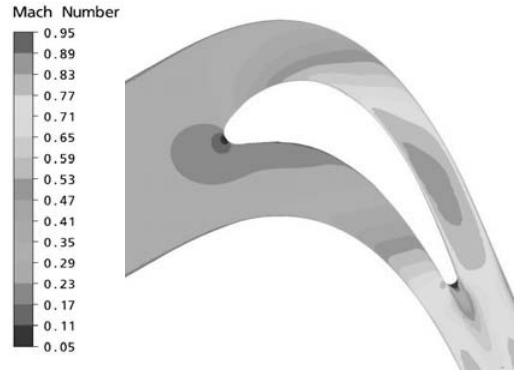

(b)

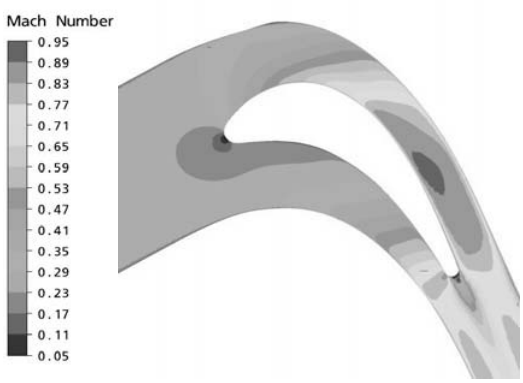

(c)

Fig. 10. Comparison of Mach number contours within a passage (a) infinite cascade flow (b) passage from the initial wall (c) passage designed with the genetic algorithm.

5. Conclusions

In order to develop a linear cascade experimental apparatus with only a single-blade without any suction bleed devices or adjustable tailboards to achieve the same flow patterns that is obtained with an infinite cascade flow condition, sidewalls were designed using an optimization method with fourteen design variables which could control the sidewall shape. The SIMN distribution was adopted as the desired variable to demonstrate periodic flow conditions. In the passage designed with the genetic algorithm, the computed SIMN on the pressure surface of the blade matched well with the target SIMN obtained with the periodic flow condition but there was a minute discrepancy on the suction surface. A better matched SIMN on the suction surface could be obtained by applying more design variables. The flow structures within the passages were illustrated using the Mach number contours. The Mach number contours within the inverse designed passage matched well with those obtained with the periodic flow condition. This design method for the sidewall could be applied to develop a cascade experimental apparatus which uses only one or a few cascade blades without the tedious work required to establish infinite cascade flow conditions.

Acknowledgment

The authors would like to acknowledge the financial support offered by grant (No. KRF-2008-005-J01001) from the Korea Research Foundation Grant and a grant (CH3-101-04) from the Carbon Dioxide Reduction & Sequestration Research Center, one of the 21st Century Frontier Programs funded by the Ministry of Education, Science and Technology funded by the Korean government.

Nomenclature

c	: Blade chord
H^*	: Objective function
$\vec{X}$	: Design variables
x, y	: Cartesian coordinates
y^+	: Non-dimensional wall unit

Greek

Γ	: Blade coordinate (x or y/c)
τ	: Surface isentropic Mach number
ω	: Weighing function

Subscripts

inf	: Periodic flow condition
suc	: Suction surface
pre	: Pressure surface
X, Y	: x- and y-direction

Abbreviations

SIMN	: Surface isentropic Mach number distribution
MMFD	: Modified method of feasible direction

References

[1] B. Ozturk and M. T. Schoberi, Effect of Turbulence Intensity and Periodic Unsteady Wake Flow Condition on Boundary Layer Development, Separation, and Reattachment Along the Suction Surface of a Low-Pressure Turbine Blade, *J. of Fluid Engineering*, 129 (2007) 747-763.

[2] M. Bloxham, D. Riemann, K. Crapo, J. Pluim and J. P. Bons,

Synchronizing Separation Flow Control with Unsteady Wakes in a Low-Pressure Turbine Cascade, *ASME Turbo Expo*, Montreal, Canada, (2007) GT2007-27525.

[3] R. D. Stiger and H. P. Hodson, The Transition Mechanism of Highly Loaded Low-Pressure Turbine Blades, *J. of Turbomachinery*, 126 (2004) 536-543.

[4] L. W. Griffin, D. J. Dorney, F. W. Huber, K. Tran, W. Shyy and N. Papila, Detailed Aerodynamic Design Optimization of an RLV Turbine, *37th AIAA/ASME/SAE/ASEE joint Propulsion Conference*, (2001) AIAA-2001-3397.

[5] S. S. Talya, A. Chattopadhyay and J. N. Rajadas, Multidisplinary Design Optimization Procedure for Improved Design of a Cooled Gas Turbine Blade, *Engineering Optimization*, 34 (2) (2002) 175-194.

[6] T. Mengistu and W. Ghaly, Single and Multipoint Shape Optimization of Gas Turbine Blade Cascades, *10th AIAA/ISSMO Multidisplinary Analysis and Optimization Conference*, Albany, New York, (2004) AIAA-2004-4446.

[7] S. Y. Cho, E. S. Yoon and B. S. Choi, A Study on a Axial-Type 2-D Turbine Blade Shape for Reducing the Blade Profile Loss, *KSME int. J.*, 16 (8) (2002) 1154-1164.

[8] R. Dornberger, P. Stoll, D. Buche and A. Neu, Multidisciplinary Turbomachinery Blade Design Optimization, (2000) AIAA-2000-0838.

[9] P. A. Giess and F. Kost, Detailed Experimental Survey of the Transonic Flow Field in a Rotating Turbine Cascade, *In 2nd European Conference on Turbomachinery-Fluid Dynamics and Thermodynamics*, Belgium, (1997).

[10] H. Lang, T. Morck and J. Woisetschlager, Stereoscopic Particle Image Velocimetry in a Transonic Turbine Stage, *Experiment in Fluids*, 32 (2002) 700-709.

[11] Y. I. Yun, L. Porreca, A. I. Kalfas, S. J. Song and R. S. Abhari, Investigation of 3-D Unsteady Flows In a Two-Stage Shrouded Axial Turbine Using Stereoscopic PIV and FRAP-Part II; Kinematics of Shroud Cavity Flow, *ASME Turbo Expo*, Barcelona, Spain, (2006) GT2006-91020.

[12] X. J. Yu and B. J. Liu, Stereoscopic PIV Measurement of Unsteady Flows in an Axial Compressor Stage, *Experimental Thermal and Fluid Science*, 31 (8) (2007) 1049-1060.

[13] M. T. Schobeiri and K. Pappu, Experimental Study on the Effect of Unsteadiness on Boundary Layer Development on a Linear Turbine Cascade, *Experiment in Fluids*, 23 (1997) 306-316.

[14] R. W. Kaszeta and T. W. Simon, Experimental Investigation of Transition to Turbulence as Affected by Passing Wakes, *NASA Contractor Report*, NASA-CR-2002-212104, Cleveland (2002).

[15] R. D. Stiger, D. Hollis and H. P. Hodson, Unsteady Surface Pressure Due to Wake-Induced Transition in a Laminar Separation Bubble on a Low-Pressure Cascade, *J. of Turbomachinery*, 126 (2004) 544-550.

[16] G. M. Laskowski, A. Vicharelli, G. Medic, C. J. Elkin, J. K. Eaton and P. A. Durbin, Inverse Design of and Experimental Measurements in a Double-Passage Transonic Turbine Cascade Model, *J. Turbomachinery*, 127 (2005) 619-626.

[17] R. Kiock, F. Lehthaus, N. C. Baines and C. H. Sieverding, The Transonic Flow Through a Plane Turbine Cascade as Measured in Four European Wind Tunnels, *J. Engineering for Gas Turbines and Power*, 108 (1986) 277-284.

[18] C. H. Cho, S. Y. Cho, C. Y. Kim and K. Y. Ahn, Design of a 160% Pitch passage Using Optimization Methods for Cascade Experiments with a Single Blade, *Engineering Optimization*, 42 (2010) 253-269.

[19] Visual DOC Reference Manual Version 6.0, Vanderplaats R&D Inc. (2006).

[20] CFX-11, version 11. ANSYS Inc. (2007).

[21] C. H. Cho, S. Y. Cho, S. E. Gorrell, K. Y. Ahn and C. Y. Kim, Inverse Design of a Double-Passage for Infinite Cascade Model Experiment, *J. of Mechanical Engineering Science*, 224 (2010) 157-168.

Chong-Hyun Cho obtained his M. S. and Ph.D. degrees from Gyeongsang National University, Korea, in 2006 and 2010. Dr. Cho is currently a Research Professor at RECAPT in Gyeongsang National University, Korea. Dr. Cho's research interests include turbomachinery design, CFD, wind tunnel test and experiment.

Kook-Young Ahn obtained his Ph.D. degree from the Department of Mechanical Engineering, KAIST, Korea, in 1994. Currently, he is a Principal Researcher in the Environment & Energy Research Division at Korea Institute of Machinery & Materials (KIMM). Also, He is the Head Professor of the Faculty of Environmental System Engineering at University of Science & Technology (UST).

Young-Cheol Kim obtained his Ph.D. degree from the Department of Mechanical Engineering, KAIST, Korea, in 2008. Currently, he is a Principal Researcher in the System Engineering Research Division at Korea Institute of Machinery & Materials (KIMM).

Soo-Yong Cho obtained his Ph.D. degrees from Case Western Reserve University, USA in 1992. Dr. Cho is currently a Professor at the Department of Mechanical and Aerospace Engineering, Gyeongsang National University, Jinju, Korea. Dr. Cho's research interests include turbomachinery, energy conversion, CFD and experiment.